Thermochimica Acta 512 (2011) 49–54

Contents lists available at ScienceDirect

Thermochimica Acta

journal homepage: www.elsevier.com/locate/tca

Solid–liquid equilibrium and thermochemical studies of organic analogue of metal–nonmetal system: Succinonitrile–pentachloronitrobenzene

Shiva Kant, R.N. Rai*

Department of Chemistry, Banaras Hindu University, Varanasi 221005, India

ARTICLE INFO

Article history:
Received 3 June 2010
Received in revised form 12 August 2010
Accepted 28 August 2010

Keywords:
Phase diagram
Thermochemistry
Organic monotectic
Solid–liquid interfacial energy
Microstructure

ABSTRACT

The phase diagram of an organic analogue of a metal–nonmetal system, involving succinonitrile–pentachloronitrobenzene, shows the formation of a eutectic and a monotectic. The two immiscible liquid phases are in equilibrium with a single liquid phase and the consolute temperature being 53.5 °C above the monotectic horizontal. The phase equilibrium study confirms the alloy composition of monotectic and eutectic at 0.150 and 0.985 mol fractions of succinonitrile, respectively. The solidification behaviour shows the validity of Hilling–Turnbull equation. The thermal properties such as heat of mixing, entropy of fusion, roughness parameter, interfacial energy, grain boundary energy and excess thermodynamic functions for parent components, monotectic and eutectic have been studied using their enthalpy of fusion values. The effects of solid–liquid interfacial energy on morphological change of monotectic have also been discussed. The microstructure of monotectic shows the lamellar growth along with droplets, however, eutectic infers the vertical growth of lamella.

© 2010 Elsevier B.V. All rights reserved.

1. Introduction

The synthesis and solidification behaviour study of monotectic alloys are of potential importance for fundamental understanding as well as for industrial applications [1–2] such as development of self-lubricating alloys. Although, metallic systems, giving monotectic alloys, constitute an interesting area of investigations [3–5], they are not suitable for detail study due to high transformation temperature, opacity, limited choice of material, difficulties in their purification and wide density difference of the components involved. In view of these difficulties, it was worth for searching some transparent organic materials of low transformation temperature, wider choice, minimised convection effects and possibility of visual observations during the solidification process. These are the special features that have prompted a number of research groups [6–8] to work on organic eutectics, monotectics and molecular complexes. The organic systems, which could be simulated as metallic systems [9–11], are used as model systems for detailed investigation of the parameters that control the mechanism of solidification and subsequently decide the properties of materials. The organic systems have also been investigated for their various physicochemical properties as well as for non-linear optical, electro-optic and different electronic applications [12–14].

The monotectic alloys have been less studied due to several difficulties associated with the systems while some of the articles explain various interesting phenomenon of monotectic alloys [2,15,16]. The problem arises due to a wide freezing range and large density difference between two liquid phases. The role of wetting behaviour, interfacial energy, thermal conductivity and buoyancy in a phase separation process has been the subject of great discussion for monotectic systems. The pentachloronitrobenzene (PCNB) is a material of high entropy of fusion and simulates the nonmetallic solidification where as succinonitrile (SCN) is a material of low entropy of fusion and corresponds the metallic solidification. Therefore, the present PCNB–SCN system may be considered as a suitable analogue of metal–nonmetal system such as Al–Si and Al–Be. In present communication, the details concerning phase diagram, thermochemistry, linear velocity of crystallization at different undercoolings, interfacial energy, grain boundary energy and microstructural investigations of PCNB–SCN system are reported.

2. Experimental

2.1. Materials and purification

The starting materials, succinonitrile and pentachloronitrobenzene, of 99% purity were obtained from Sigma–Aldrich, Germany. Succinonitrile was purified by repeated distillation under reduced pressure while pentachloronitrobenzene was used as received. The melting temperatures of both compounds were found to be in agreement with the values reported in literature [17].

* Corresponding author at: Department of Chemistry, Faculty of Science, Banaras Hindu University, Varanasi, U.P. 221005, India. Tel.: +91 542 6701597; fax: +91 542 2368127.
E-mail address: rn_rai@yahoo.co.in (R.N. Rai).

0040-6031/$ – see front matter © 2010 Elsevier B.V. All rights reserved.
doi:10.1016/j.tca.2010.08.021

2.2. Phase diagram

The phase diagram of PCNB–SCN system was determined by the thaw-melt method in the form of temperature–composition curve. In this method [18,19] the mixtures of two components in different compositions were taken in sealed test tube and these mixtures were homogenized by repeating the process of melting and mixing followed by chilling in ice cooled water 4–5 times. The melting points of different miscible compositions were determined using a melting point apparatus (Toshniwal melting point) attached with a precision thermometer associated with an accuracy of ±0.5 °C, while the miscibility temperatures of compositions showing miscibility gap were noted from the temperature controlled silicon oil bath.

2.3. Enthalpy of fusion

The values of heat of fusion of the pure components, the eutectic and the monotectic were determined [20] by differential scanning calorimeter (Mettelar DSC-4000 system). Indium and zinc samples were used to calibrate the system and the amount of test samples and heating rate were about 5 mg and 10 °C min^{-1}, respectively. The values are reproducible within ±1.0%.

2.4. Growth kinetics

The solidification behaviour of pure components, monotectic and the eutectic were studied by determining the linear velocity of crystallization at different undercoolings [21,22]. Molten samples were separately taken in a U-shaped glass tube of about 150 mm horizontal portion and 5 mm internal diameter and tube was placed in a silicone oil bath. The temperature of oil bath was maintained using microprocessor temperature controller of accuracy ±0.5 °C. At different undercoolings, a seed crystal of the same composition was added to start nucleation, and the rate of movement of the solid–liquid interface was measured using a traveling microscope and a stop watch.

2.5. Microstructure

Microstructures of the pure components, the eutectic and the monotectic were recorded [18] by placing a drop of molten compound on a hot glass slide. To avoid the inclusion of the impurities from the atmosphere, the melt was covered by a cover slip. The melt was allowed to cool to get a super cooled liquid. A seed crystal of the same composition was used at one end to start the nucleation and care was taken to have unidirectional freezing. The unidirectional solidify microstructure thus developed was placed on the platform of an optical (Leitz Labourlux D) microscope. Different regions were viewed and the photographs of the interesting regions were taken with suitable magnification with the help of camera attached with the microscope.

3. Results and discussions

3.1. Phase diagram

The phase diagram of PCNB–SCN system, established in their melting/miscibility temperature and composition, shows the formation of a monotectic and a eutectic as depicted in Fig. 1, however, the numerical data is tabulated in Table 1. Melting point of PCNB (145.0 °C) decreases by the addition of SCN. When the mole fraction of SCN is 0.15, the immiscibility appears and at certain temperature these two immiscible liquids are completely miscible. With an increase in composition of SCN the miscibility temperature increases and it attains the maximum values where the mole fraction of SCN is 0.60. This maximum miscibility temperature is known as critical or upper consolute temperature (T_c, 192.0 °C) which is 53.5 °C above the monotectic horizontal (M_h). The both

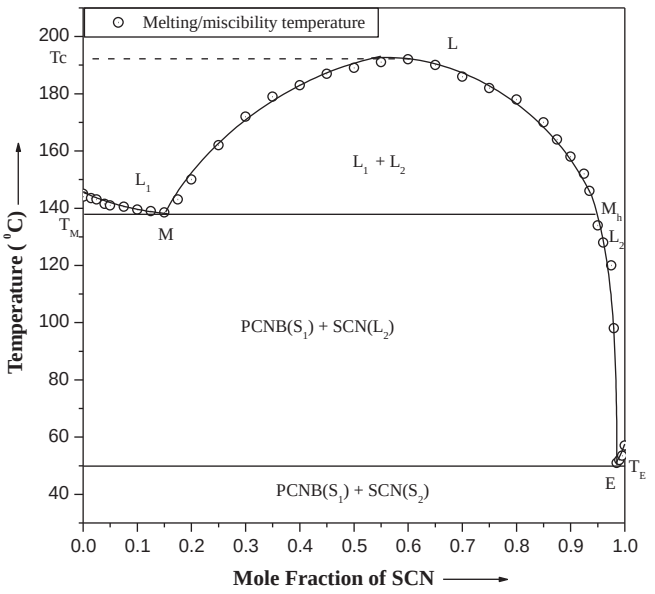

Fig. 1. Phase diagram of pentachloronitrobenzene–succinonitrile system. (○) Melting/miscibility temperature.

Table 1
Compositions of succinonitrile (SCN) and pentachloronitrobenzene (PCNB) and its respective melting/miscibility temperature.

Mole fraction of SCN (±0.0002 M)*	Mole fraction of PCNB (±0.0002 M)*	Melting/miscibility temperature
0.000	1.000	145.0
0.010	0.990	144.0
0.015	0.985	143.5
0.025	0.975	143.0
0.040	0.960	141.5
0.050	0.950	141.0
0.075	0.925	140.5
0.100	0.900	139.5
0.125	0.875	139.0
0.150	0.850	138.5
0.175	0.825	139.5
0.200	0.800	150.0
0.250	0.750	162.0
0.300	0.700	172.0
0.350	0.650	179.0
0.400	0.600	183.0
0.450	0.550	187.0
0.500	0.500	189.0
0.550	0.450	191.0
0.600	0.400	192.0
0.650	0.350	190.0
0.700	0.300	186.0
0.750	0.250	182.0
0.800	0.200	178.0
0.850	0.150	170.0
0.875	0.125	164.0
0.900	0.010	158.0
0.925	0.075	152.0
0.935	0.065	146.0
0.950	0.050	134.0
0.960	0.040	128.0
0.975	0.025	120.0
0.980	0.020	98.0
0.985	0.015	51.0
0.990	0.010	52.0
0.995	0.005	53.5
1.000	0.000	57.0

* The possible variation in mol fraction.

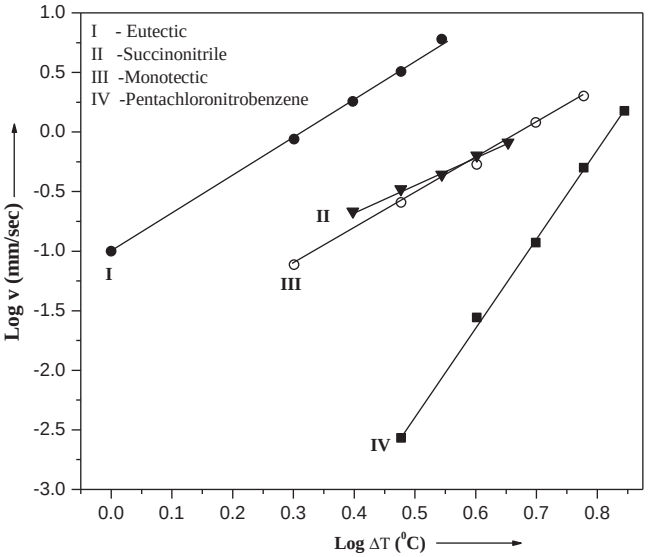

Fig. 2. Linear velocity of crystallisation at various degrees of undercooling for pentachloronitrobenzene, succinonitrile and their eutectic and monotectic.

components, in any proportions, are miscible above the critical temperature. The inference of thermal change on different compositions reveals that there are three reactions of interest, which occur isothermally on solidification. The first reaction is concerns with phase separation where a single liquid phase separates in two liquid phases at the critical temperature, and can be written as

$$L \rightarrow L_1(\text{rich in PCNB}) + L_2(\text{rich in SCN})$$

The direct observation on kinetics of phase separation from liquid L to $L_1 + L_2$ is interesting but the mechanism appears to be quite complicated. The disturbance in the whole liquid is observed which might be the consequence of collision between droplets, diffusion and movement by buoyancy driven fluid flow. A small decrease in temperature from the critical solution temperature (192.0 °C) is quite enough for the phase separation process to occur within few seconds. For metallic systems the numbers of possibilities [20,21] such as tendencies of compound formation, atomic radii difference, the valences differences of the components. At least one of these possibilities might be responsible for the occurrence of the miscibility gap in the liquid state.

The second reaction, known as monotectic reaction, concern with cooling of monotectic composition from monotectic temperature, the liquid dissociates to give a solid and a liquid according to the following monotectic reactions:

$$L_1(\text{rich in PCNB}) \rightarrow S_1(\text{rich in PCNB}) + L_2(\text{rich in SCN})$$

The third reaction is the eutectic reaction in which the liquid L_2 of eutectic composition is cooled below the eutectic horizontal; the liquid decomposes to give two solids as

$$L_2(\text{rich in SCN}) \rightarrow S_1(\text{rich in PCNB}) + S_2(\text{rich in SCN})$$

The monotectic, the eutectic and the critical solution temperatures are 138.5, 51.0 and 192.0 °C, respectively.

3.2. Growth kinetics

In order to study the crystallization behaviour of the pure components, the eutectic and monotectic the crystallization rate (v) are determined at different particular undercoolings (ΔT) by measuring the rate of movement of solid–liquid interface in a capillary. The plots between $\log \Delta T$ and $\log v$ are given in Fig. 2 and the linear dependence of these plots are in accordance with the Hillig and Turnbull equation [23]:

$$v = u(\Delta T)^n \quad (1)$$

where u and n are the constant and depending on the nature of the materials. The values of u and n in each case were determined from the intercepts and slope of the straight lines (Fig. 2) and given in Table 2. The crystallisation of eutectic/monotectic begins with the formation of the nucleus of one of the phases. This phase grows until the surrounding liquid becomes rich in the other component and a stage is reached when the second component start nucleating. Whether further crystallization will proceed following the alternate nucleation mechanism or side-by-side growth mechanism is decided by the value of u, which is measure of the rate of solidification of the eutectic and monotectic. When u value of eutectic/monotectic is less than that of the components, the solidification takes place by the alternate nucleation mechanism. On the other hand when the value of u is more than that of both components or lies in between that of the components, the solidification takes place by side-by-side mechanism. The value of u (Table 2) infers that growth velocity of monotectic lies between those of the parent components; however for eutectic it is higher than the parent components. These findings suggest that the two phases of monotectic and eutectic solidify by the side-by-side growth mechanism [24].

Table 2
Values of n and u for pure components, monotectic and eutectic.

Material	n	u (mm s^{-1} deg^{-1})
PCNB	7.4	8.4×10^{-7}
SCN	3.0	2.7×10^{-2}
Monotectic	2.9	9.7×10^{-3}
Eutectic	3.2	9.7×10^{-2}

4. Thermochemistry

4.1. Enthalpy of fusion

The values of enthalpy of fusion of the pure components, the eutectic and the monotectic, determined by the DSC method, are reported in Table 3. For comparison, the value of enthalpy of fusion of eutectic calculated by the mixture law [18] is also included in the same table. The enthalpy of mixing which is the difference of experimentally determined and the calculated values of the enthalpy of fusion was found to be -1.7 kJ mol^{-1}. As such, three types of structures are suggested; quasi-eutectic for $\Delta_{mix}H > 0$, clustering of molecules for $\Delta_{mix}H < 0$ and molecular solution for $\Delta_{mix}H = 0$. The negative value of $\Delta_{mix}H$ for the eutectic suggests the clustering of molecules in the binary melt of the eutectic [25]. The entropy of fusion ($\Delta_{fus}S$) values has been calculated by dividing the enthalpy of fusion values by their corresponding absolute melting temperatures (Table 3). In all the cases, the entropy of fusion being positive suggests an increase in randomness of the system during

Table 3
Heat of fusion, heat of mixing, entropy of fusion and roughness parameter of pure components and their monotectic and eutectic.

Materials	Heat of fusion (kJ mol^{-1})	Heat of mixing (kJ mol^{-1})	Entropy of fusion (J mol^{-1} K^{-1})	Roughness parameter (α)
PCNB	19.2		45.8	5.5
SCN	3.7		11.2	1.4
Monotectic	16.8		41.0	4.9
Eutectic (Exp.)	2.2	−1.7	6.7	0.8
(Cal.)	3.9			

Table 4
Interfacial energy of pentachloronitrobenzene, succinonitrile and their eutectic and monotectic.

Parameter	Interfacial energy ($J\,m^{-2}$)	Grain boundary energy (γ) ($J\,m^{-2}$)
σ_{SL_2} (SCN)	9.34×10^{-3}	18.68×10^{-3}
σ_{SL_1} (PCNB)	29.35×10^{-3}	58.70×10^{-3}
$\sigma_{L_1L_2}$ (PCNB–SCN)	5.58×10^{-3}	11.15×10^{-3}
σ_E (PCNB–SCN)	9.64×10^{-3}	19.28×10^{-3}

melting. The lowest value of the entropy of fusion for the eutectic indicates the least effectiveness of entropy factor in the melting of the eutectic.

4.2. Size of critical nucleus and interfacial energy

When a melt is cooled below its melting temperature, the liquid phase does not solidify spontaneously because, under equilibrium condition, the melt contains number of clusters of molecules of different sizes. As long as the clusters are well below the critical size [24], they can not grow to form crystals and, therefore, no solid would result. The critical size (r^*) of nucleus is related to interfacial energy (σ) by the equation:

$$r^* = \frac{2\sigma T_{fus}}{\Delta_{fus}H\,\Delta T} \tag{2}$$

where T_{fus}, $\Delta_{fus}H$ and ΔT are melting temperature, heat of fusion, and degree of undercooling, respectively. An estimate of the interfacial energy is given by the expression:

$$\sigma = \frac{C\Delta_{fus}H}{(N_A)^{1/3}(V_m)^{2/3}} \tag{3}$$

where N_A is the Avogadro number, V_m is the molar volume, and parameter C lies between 0.30 and 0.35. The calculated values of interfacial energy for different materials and critical size of nucleus at different undercoolings are reported in Tables 4 and 5, respectively.

4.3. Grain boundary energy

The grain boundary energy (γ) could be estimated with help of interfacial energy for the determination of grain boundary energy between different interfaces, the expression used is

$$\gamma = 2\sigma_{SL}\cos\theta \tag{4}$$

where θ is the angle between tangent on interface. The determination of the exact value of θ is complicated in present system. However, the range of grain boundary energy could be studied because the value of $\cos\theta$ may be less than or equal to one, and thus the value of grain boundary energy will be less than or equal to twice of interfacial energy. The maximum grain boundary energy for different possible interfaces in present system have been estimated and given in Table 4.

Table 5
Critical radius of succinonitrile, pentachloronitrobenzene and their eutectic and monotectic.

Undercooling ΔT (°C)	Critical radius $\times 10^8$ (cm)			
	SCN	PCNB	Monotectic	Eutectic
1.0			2.7	28.7
2.0			1.3	14.4
2.5	6.8			
3.0	5.7	4.3	0.91	9.6
3.5	4.9			
4.0	4.3	3.2	0.68	7.2
4.5	3.8			
5.0		2.6	0.54	5.7
6.0		2.1		
7.0		1.8		

Table 6
Excess thermodynamic functions for the eutectic.

Material	g^E ($kJ\,mol^{-1}$)	h^E ($kJ\,mol^{-1}$)	s^E ($kJ\,mol^{-1}\,K^{-1}$)
Eutectic	0.0790	0.5300	0.0014

4.4. Excess thermodynamic functions

The deviation from the ideal behaviour can best be expressed in terms of excess thermodynamic functions, namely, excess free energy (g^E), excess enthalpy (h^E), and excess entropy (s^E) which give a more quantitative idea about the nature of molecular interactions. The excess thermodynamic functions could be calculated [24,26] by using the following equations and the values are given in Table 6:

$$g^E = RT\left[x_1 \ln\gamma_1^l + x_2 \ln\gamma_2^l\right] \tag{5}$$

$$h^E = -RT^2\left[x_1\frac{\partial \ln\gamma_1^l}{\partial T} + x_2\frac{\partial \ln\gamma_2^l}{\partial T}\right] \tag{6}$$

$$s^E = -R\left[x_1 \ln\gamma_1^l + x_2 \ln\gamma_2^l + x_1T\frac{\partial \ln\gamma_1^l}{\partial T} + x_2T\frac{\partial \ln\gamma_2^l}{\partial T}\right] \tag{7}$$

where $\ln\gamma_i^l$, x_i and $\partial \ln\gamma_i^l/\partial T$ are activity coefficient in liquid state, the mole fraction and variation of log of activity coefficient in liquid state as function of temperature of a component i.

It is evident from Eqs. (5)–(7) that activity coefficient and its variation with temperature are required to calculate the excess functions. Activity coefficient (γ_i^l) could be evaluated [19,25] by using the equation:

$$-\ln(x_i\,\gamma_i^l) = \frac{\Delta_{fus}H_i}{R}\left(\frac{1}{T_{fus}} - \frac{1}{T_i}\right) \tag{8}$$

where x_i, $\Delta_{fus}H_i$, T_i and T_{fus} are mole fraction, enthalpy of fusion, melting temperature of component i and eutectic melting temperature, respectively. The variation of activity coefficient with temperature could be calculated by differentiating Eq. (8) with respect to temperature:

$$\frac{\partial \ln\gamma_i^l}{\partial T} = \frac{\Delta_{fus}H_i}{RT^2} - \frac{\partial x_i}{x_i\partial T} \tag{9}$$

In this expression $\partial x_i/\partial T$ have been evaluated by taking two points near the eutectic. The calculated values of different thermodynamic functions have been given in Table 6. The positive values of excess free energy indicate that there is an associative interaction between like molecules [27].

4.5. Microstructure

In general microstructure gives information about shape and size of the crystallites, and distribution of the phases which play a very significant role in deciding about mechanical, electrical, magnetic and optical properties of materials. Thermal conductivity, entropy of fusion solid liquid interface are the materials' properties and undercooling, growth velocity and temperature gradient along interface are the physical parameters, however these are important to control the mechanism of microstructure [28,29]. According to Hunt and Jackson [30] the type of growth from melts depends upon the interface roughness (α) defined by

$$\alpha = \frac{\xi\Delta_{fus}H}{RT} \tag{10}$$

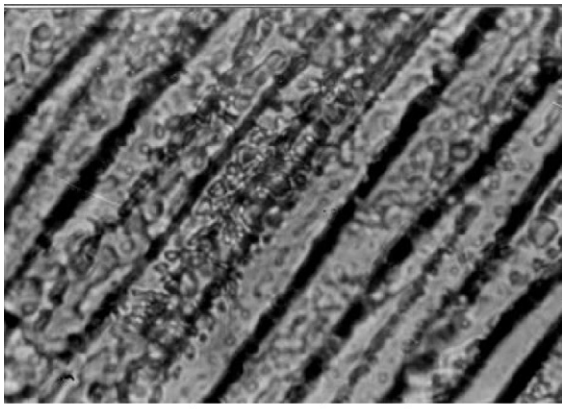

(a) Microstructure of monotectic

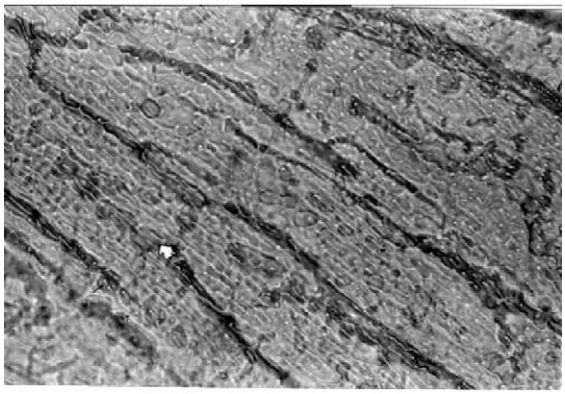

(b) Microstructure of monotectic

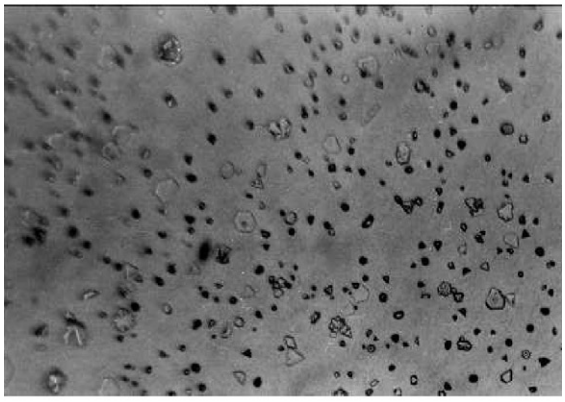

(c) Microstructure of eutectic

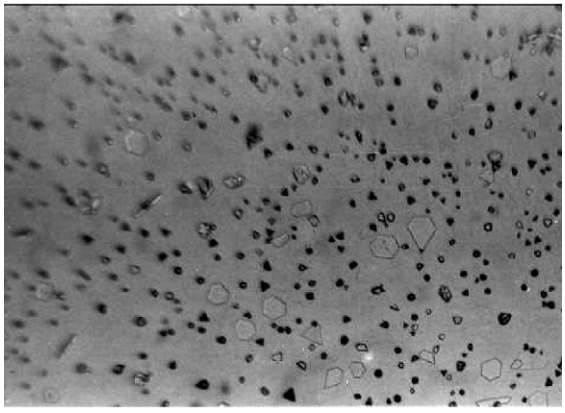

(d) Microstructure of eutectic

Fig. 3. Optical microphotograph of directionally solidify: (a) and (b) monotectic, and (c) and (d) eutectic.

where ξ is a crystallographic factor which is generally equal to or less than one. The values of α are reported in Table 3. If $\alpha > 2$ the interface is quite smooth and the crystal develops with a faceted morphology. On the other hand, if $\alpha < 2$, the interface is rough and many sites are continuously available and the crystal develops with a non-faceted morphology.

4.5.1. The microstructure and growth of monotectic and eutectic

In monotectic solidification when liquid of monotectic composition (Fig. 1) is allowed to cool, below the monotectic temperature (T_m), the stability of two liquid phases L_1 and L_2 and a solid phase, S, at the solid–liquid interface are required [17]. The necessary conditions for the stable three phases in contact have been explained by Chadwick [29]. Whether droplets nucleate in the melt or on the solid–liquid interface depends on the relative magnitude of the three interfacial energies. The condition required for the balance of interfacial energies is as fallows:

$$\sigma_{SL_2} \leq \sigma_{SL_1} + \sigma_{L_1L_2} \tag{11}$$

and

$$\sigma_{SL_2} \geq \sigma_{SL_1} + \sigma_{L_1L_2} \tag{12}$$

where σ_{SL_1}, σ_{SL_2} and $\sigma_{L_1L_2}$ are the interfacial energies of solid (S) and the liquid L_1, solid (S) and the liquid L_2, and liquids L_1 and liquid L_2, respectively. The surface energies were calculated [11], and have been tabulated in Table 4. The interfacial energy of SCN has compared with the reported value [19,31]. The wetting conditions discussed by Cahn [32] could be successfully applicable to the present system as the interfacial energies are related by the relation:

$$\sigma_{SL_2} < \sigma_{SL_1} + \sigma_{L_1L_2}$$

The finding Indicate that the liquid (L_1) wets the solidified PCNB perfectly. The directionally solidified optical microphotographs of monotectic have shown in Fig. 3(a) and (b). Fig. 3(a) shows lamellar growth of one of the phases whereas droplets of another phase have elongated and solidify with lamella. The closer view of structure infers trapping of droplets on lamella. On the other hand, the microstructure of monotectic solidified with faster rate (Fig. 3(b)) shows broken and branched lamellar morphology, the elongation of droplets could also be observed for another phase.

The microstructures of eutectic have given in Fig. 3(c) and (d). It seems the growth of eutectic microstructure has taken place vertically. The top view of both, Fig. 3(c) and (d), microstructures predict lamellar growth morphology which would have grown vertically. The observations of microstructures are interesting where different (circular, trigonal, rectangular, pentagonal and hexagonal) shapes could be noticed.

5. Conclusions

The phase diagram studies of pentachloronitrobenzene–succinonitrile shows the formation of a monotectic and a eutectic at particular compositions where mole fractions of succinonitrile are 0.150 and 0.985, respectively. The diagram shows large miscibility gap region and the consolute temperature was found to be 53.5 °C above the monotectic horizontal. The solidification behaviour of pure components, the eutectics and the monotectic studied at different undercooling suggest that growth takes place according to the Hillig–Turnbull equation. The thermal study of the pure components, the binary monotectic and eutectic were studied using DSC. Utilizing heat of fusion value, the various thermal properties such as entropy of fusion, enthalpy of mixing, excess thermodynamic functions, interfacial energy and grain boundary energy were studied and have been reported

for pure and binary materials. The interfacial energies satisfy the relation $\sigma_{SL_2} < \sigma_{SL_1} + \sigma_{L_1L_2}$ that infers the applicability of Cahn wetting condition to the present system. The microstructural investigations show the lamellar and broken lamellar growth morphology along with droplets for monotectic alloy, and the growth morphology for the eutectic has indicated the growth of lamellas of different shapes which have probably grown vertically.

Acknowledgements

Authors are thankful to the Board of Research in Nuclear Science, BARC, Mumbai, India, for financial support and also to Head, Department of Chemistry, Banaras Hindu University, Varanasi, India for providing the infrastructure facilities.

References

[1] R.N. Gruggel, A. Hellawel, Metall. Trans. A 12(A) (1981) 669–681.
[2] D.M. Herlach, R.F. Cochrane, I. Egry, H.J. Fecht, A.L. Greer, Int. Mater. Rev. 38 (1993) 273–347.
[3] R. Trivedi, W. Kurz, Int. Mater. Rev. 32 (1994) 49–74.
[4] B. Majumdar, K. Chattopadhyay, Metall. Trans. A 27(A) (1996) 2053–2057.
[5] M.E. Glicksman, N.B. Singh, M. Chopra, Manuf. Space 11 (1982) 207–218.
[6] J. Seth, W.R. Wilcox, J. Cryst. Growth 114 (1991) 357–363.
[7] J. Teng, S. Liu, J. Cryst. Growth 290 (2006) 248–257.
[8] L. Sturz, V.T. Witusiewicz, U. Hecht, S. Rex, J. Cryst. Growth 270 (2004) 273–282.
[9] U.S. Rai, R.N. Rai, J. Cryst. Growth 191 (1998) 234–242.
[10] S. Kant, R.S.B. Reddi, R.N. Rai, Fluid Phase Equilib. 291 (2010) 71–75.
[11] U.S. Rai, R.N. Rai, J. Cryst. Growth 169 (1996) 563–569.
[12] J.P. Farges, Organic Conductors, Marcel Dekker, Inc., New York, 1994.
[13] P. Gunter, Nonlinear Optical Effects and Materials, Springer-Verlag, Berlin, 2000.
[14] N.B. Singh, T. Henningsen, R.H. Hopkins, R. Mazelsky, R.D. Hamacher, E.P. Supertzi, F.K. Hopkins, D.E. Zelmon, O.P. Singh, J. Cryst. Growth 128 (1993) 976–980.
[15] J. Glazer, Int. Mater. Rev. 40 (1995) 65–93.
[16] A. Ecker, D.O. Frazier, J.I.D. Alexander, Metall. Trans. 20A (1989) 2517–2527.
[17] J.A. Dean, Lange's Handbook of Chemistry, McGraw-Hill, New York, 1985.
[18] R.N. Rai, J. Mater. Res. 19 (5) (2004) 1348–1355.
[19] U.S. Rai, R.N. Rai, Chem. Mater. 11 (11) (1999) 3031–3036.
[20] J.W. Dodd, K.H. Tonge, Thermal methods, in: B.R. Currel (Ed.), Analytical Chemistry by Open Learning, Willey, New York, 1987, p. 120.
[21] R.S.B. Reddi, S. Kant, U.S. Rai, R.N. Rai, J. Cryst. Growth 312 (2009) 95–99.
[22] R.N. Rai, U.S. Rai, Thermochim. Acta 387 (2002) 101–107.
[23] W.B. Hillig, D. Turnbull, J. Chem. Phys. 24 (1956) 914.
[24] U.S. Rai, R.N. Rai, J. Therm. Anal. 53 (1998) 883–893.
[25] R.N. Rai, U.S. Rai, Thermochim. Acta 363 (2000) 23–28.
[26] J.W. Christian, The Theory of Phase Transformation in Metals and Alloys, Pergamon Press, Oxford, 1965, p. 992.
[27] N. Singh, N.B. Singh, U.S. Rai, O.P. Singh, Thermochim. Acta 95 (1985) 291–293.
[28] R. Elliot, Int. Met. Rev. 22 (1997) 161–186.
[29] G.A. Chadwick, Metallography of Phase Transformations, Butterworths, London, 1972.
[30] J.D. Hunt, K.A. Jackson, Trans. Met. Soc. AIME 236 (1966) 843–852.
[31] N. Marasli, K. Keslioglu, B. Arslan, J. Cryst. Growth 247 (2003) 613–622.
[32] J.W. Cahn, J. Chem. Phys. 66 (1977) 3667–3672.